Gigacycle fatigue of bearing steels

C. Bathias*

For a practical point of view, the bearing steels are loaded up to the very high cycle fatigue regime, in service, far away from the Wöhler regime. In the present paper, several approaches are discussed in order to open some ways of investigation, in the range of 10^9 cycles: accelerated fatigue testing, thermal dissipation, fish-eye formation, inclusion effect, short crack propagation and stability of the microstructure.

This paper is part of a special issue on 'Bearing steels'

Introduction

When the fatigue curve or stress versus the number of cycles (SN) curve is defined, it is usually performed in reference to carbon steels. The SN curve is generally limited to 10^7 cycles and it is admitted, according to the standard that a horizontal asymptote allows one to determine a fatigue limit value for an alternating stress between 10^6 and 10^7 cycles. Beyond 10^7 cycles, the standard considers that the fatigue life is infinite. For other alloys, it is assumed that the asymptote of the SN curve is not horizontal.

For results of fatigue limits based on 10^9 cycles, some results can be observed in Refs. 1–8. Until now, the shape of the SN curve beyond 10^7 cycles is predicted using probabilistic method and this is also true for the fatigue limit. In principle, the fatigue limit is given for a number of cycles to failure. Using, for example, the staircase method, the fatigue limit is given by the average alternating stress σ_D and the probability of fracture is given by the standard deviation of the scatter s. Classical ways to determine the infinite fatigue life is to use a Gaussian function. Roughly speaking, it is said that $\sigma_D - 3s$ gives a probability of fracture close to zero. Assuming s is equal to 10 MPa, the true infinite fatigue limit should be $\sigma_D - 30$ MPa. However, experiments show that between σ_D for 10^6 and σ_D for 10^9 cycles, the difference is >30 MPa for many alloys.

The so called Standard Deviation (SD) approach to the average fatigue limit is certainly not the best way to reduce the risk of rupture in fatigue. Whereas one is conscious that it is only a last resort, only experience can remove this ambiguity by appealing to some tests of accelerated fatigue. Today, some piezoelectric fatigue machines are very reliable, capable of producing 10^{10} cycles in less than one week, whereas the conventional systems require more than three years of tests for only one sample. It is interesting to point out that most of the structural components are working between 10^4 and 10^{11} cycles. The fatigue life of a car engine is ranging beyond 10^8 cycles, and the large diesel engines for ships work up to 10^9 cycles. It should be realised that, currently, the technical limit for fatigue life is about 10^{10} cycles.

From an historical point of view, it was said for the first time (1984–97) by Japanese researchers,[1] that metals can fail between 10^7 and 10^8 cycles. However, the gigacycle fatigue failure in many alloys was experimentally proven very recently (1990s) up to 10^{10} cycles, by Bathias and co-workers.[2–4] Up to now, the SN curve is still assumed to be a hyperbolic function, but in reality the asymptote is not horizontal. This means that fatigue initiation mechanisms from 10^6 to 10^9 cycles is a new topic of great interest for advanced technologies and SN curves, that are not asymptotic, must be determined in order to guarantee the real fatigue strength in high cycle regime. The actual shape of the SN curve between 10^6 and 10^{10} cycles is a better way to help in the prediction of risk in fatigue cracking. Since Wöhler, the standard is to represent the SN curve by a hyperbole more or less modified as indicated below:

hyperbole $\ln N_f = \log a - \ln \sigma a$

while other methods may be listed as:

Wöhler $\ln N_f = a - b\sigma a$

Basquin $\ln N_f = a - b\ln \sigma a$

Stromeyer $\ln N_f = a - b\ln (\sigma a - c)$

Only the exploration of the life range between 10^6 and 10^{10} cycles will create a safer approach to modelling. It should not be forgotten that the fatigue strength is strongly dependant on the number of cycles chosen to stop the test.

The gigacycle fatigue regime is now investigated with the development of devices (piezoelectric machines) working at high frequency (20 or 30 kHz), allowing one to obtain 10^8 or more cycles in reasonable testing time. When the crack initiation site is in the interior, this leads to the formation of a 'fish-eye' on the fracture surface, and the origin of the fatigue crack is an inclusion, a 'super grain' (microstructural in-homogeneity), or porosity.[2] The initiation phase in the gigacycle fatigue can be described in terms of a local microstructurally irreversible portion of the cumulative plastic strain. When crack initiation appears, a short crack propagates followed by a long crack. In all cases, a cyclic plastic zone around the crack occurs leading to a high thermal dissipation. Thus, the recording of the surface

LEME, University Paris ouest, 50 rue de Sevres, Ville d'Avray 92410, France

*Corresponding author, email claude@bathias.com

temperature of the sample during the test must allow to follow the fatigue damage and to determine the number of cycles at the crack initiation.

Indeed, it is of interest to focus the investigation on the gigacycle fatigue properties of bearing steels 52 100, under push–pull loading, tension–tension loading and torsion loading. It is confirmed the influence of inclusions is a key problem. A comparison with the Japanese results using a rotating bending fatigue test and the results from research using axial loading demonstrates a difference between the obtained SN curves.

A thermal dissipation cannot be avoided during crack growth at 20 kHz. It means that the interest of the piezoelectric fatigue systems must be limited to the crack initiation in the gigacycle range and to the threshold crack regime up to the threshold corner of the Paris curve. The increase of temperature associated with a microstructural transformation seems to explain a frequency effect which does not exist for stable conditions.

Test procedure

Ultrasonic fatigue machine

The test methods for determining gigacycle fatigue properties have been developed and applied by many researchers around the world. In 1950, Mason and Wood built the first 20 kHz piezoelectric machine. Thanks to the ultrasonic fatigue technology, we can establish the typical life of a great number of components that achieve 10^9–10^{10} cycles during its life in service. For some 20 years, the authors' laboratory has carried out diverse fatigue life investigations on many materials with the use of a piezoelectric fatigue testing machine at 20 kHz, which has approved capability for producing fatigue property data in gigacycle regime.

A new piezoelectric fatigue machine with 30 kHz was used to explore the fatigue properties of bearing steel 52 100 in the domain of the 10^9–10^{11} cycles. Here, a comparison of fatigue testing with different frequencies was made. Using a 20 kHz piezoelectric fatigue machine, it takes us around 14 h to obtain 10^9 cycles, 6 days for 10^{10} cycles, and 58 days for 10^{11} cycles. The stress excitement principle is the same for both at 30 kHz as 20 kHz piezoelectric fatigue machines, where the vibration of the specimen is induced by a piezoceramic converter, which generates acoustical waves in the specimen through a power concentrator (horn) in order to obtain a desired material displacement and an amplification of the stress.[2] The resonant specimen dimension and stress concentration factor were calculated by finite element method for 20 and 30 kHz.

Fatigue tests were performed in an open environment at 20 and 30 kHz with the piezoelectric fatigue machine, using a symmetrical cyclic stress ($R=-1$), and cooling with compressed air at 20°C to keep the temperature of the specimen below 30°C. The dynamic displacement amplitude of the specimen end face is controlled by an optical sensor and computer control in order to keep the stress constant during the test. The test is automatically stopped when the frequency reduced to 19·5 kHz which is
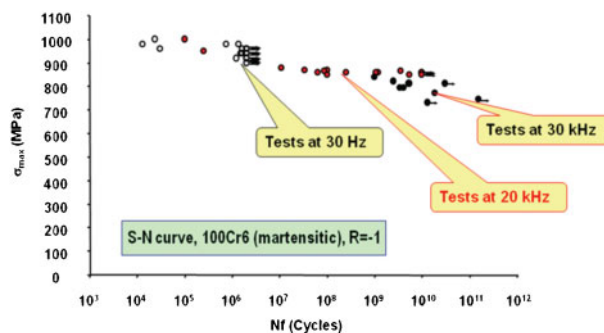
1   Gigacycle SN curve of martensitic bearing steel at different frequency and $R=-1$

attributed to cracks development before fracture. Both the specimen and machine are described in other papers.[4]

In order to test the torsion fatigue limit of the alloy up to 10^{10} cycles, an ultrasonic torsion fatigue system was designed. Attached to the transducer are two horns; one serves to amplify the longitudinal mechanical displacement, and the other to amplify the torsion angular displacement. A torsion fatigue specimen designed to run in resonance with the system is then attached to the horn. The specimens were designed so that the maximum strain is located in the minimum gage section.

Material and specimens

The smooth specimens to be tested at 20 kHz come from three different manufacturers (NF 100C6*, NF 100C6** and JIS SUJ2). These specimens have an hourglass shape with a minimum diameter of 3 mm and a radius of curvature at the reduced section (notch radius) of 31 mm). The fatigue results obtained from every group of specimens were compared in order to investigate the effect of the used processing method. The smooth specimen to be tested at 30 kHz was machined by only one manufacturer (NF 100C6*), an axisymetric specimen with a minimum diameter of 3 mm and having a hourglass shape radius of 16 mm.

Finally, the notch specimen from only one manufacturer (NF 100C6*) with a minimum diameter of 6·4 mm and 60° notch with a round notch radius of 2 mm, was used to evaluate the intrinsic resistance of the microstructure, and the thermal effect on vibratory fatigue.

The three steelmakers have manufactured the specimens independently although they have used the steels with similar chemical compositions, and applied similar heat treatments, and machining operations. The chemical composition of NF 100C6 martensitic and bainitic bearing steels is 1·0C–0·2Si–0·3Mn–0·001P–0·008S–1·4Cr–0·03Mo–0·14Ni (wt-%). Table 1 shows some measured mechanical properties for the NF 100C6 martensitic bearing steels.
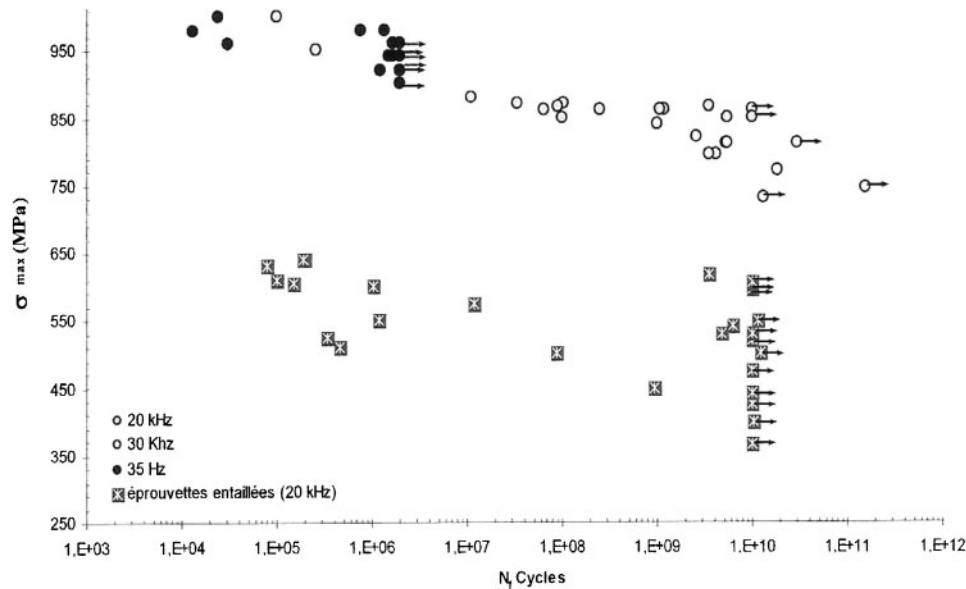
Gigacycle fatigue SN curves of bearing steels

Push pull loading

The SN curves obtained from all the fatigue tests are shown in Figs. 1–6. The main purpose of Fig. 1 is to

Table 1   Mechanical properties of tested bearing steels

	E_s/GPa	σ_y/MPa	UTS/MPa	P/kg m^{-3}	HV30	HRC
NF 100C6 martensitic	210	1158	2316	7860	778	63·2

2 Gigacyle fatigue SN curve of 100C with and without notch ($R=-1$)

confirm that the shape of the SN curve is continuously decreasing from the mega- to the gigacycle regime, without effect of frequency. No step is observed in the SN curve when the load is tension–compression and when the microstructure is stable.

The results obtained at different frequencies show that fatigue rupture can occur beyond 10^9 cycles and the difference of fatigue resistance can decrease by 150, or even 200 MPa between 10^6 and 10^{10} cycles under these conditions. The fatigue limit of bearing steels defined with a statistical analysis between 10^6 and 10^7 cycles cannot guarantee a safe design.

As to the notch specimen, fatigue resistance is far lower than for the smooth specimen, which is due to the existence of a larger stress concentration at notch surface. Again, the SN curve for the notched specimens is slowly decreasing after 10^6 cycles, if compared with the smooth specimens curve. It means that the difference between the two SN curves at 10^9 cycles is smaller than

that at 10^6 cycles (about 150 and 300 MPa), but the fatigue strength for notched specimens is ranging ~ 600 MPa. It seems that the effect of stress concentration at the tip of a notch is similar in the mega- than in the gigacycle regime (Fig. 2).

Roughly speaking, it is said that σ_f-3s gives a probability of fracture close to zero. In our testing, the standard deviation s is close to 10 MPa, the true infinite fatigue limit should be σ_f-30 MPa. Thus, we can get the fatigue limit at 10^9 cycles from the fatigue resistance at 10^6 cycles, which is calculated to be 905 MPa using the statistical method. The experimental fatigue limit at 10^{10} cycles is 809·8 MPa. This differs by 100 MPa if compared with the calculated results. Consequently, it seems that the high frequency fatigue test is the most effective way to obtain the materials fatigue strength in the high cycle regimes.

Figure 4 shows the SN curve of 100C6 steel for torsion fatigue test results at 20 kHz. Fatigue lifetime
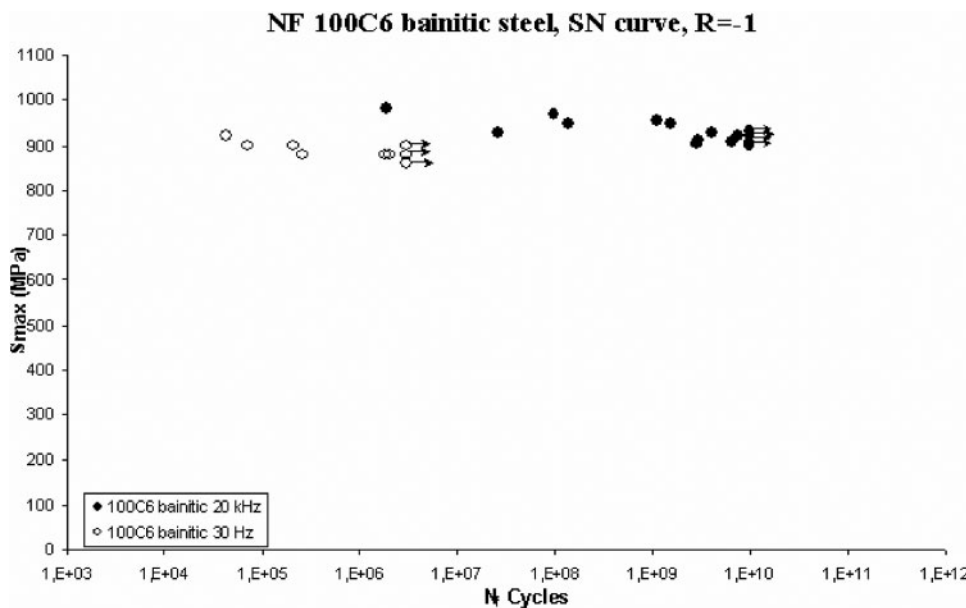
3 Gigacycle fatigue SN curve of bainitic bearing steel tension–tension ($R=-1$)
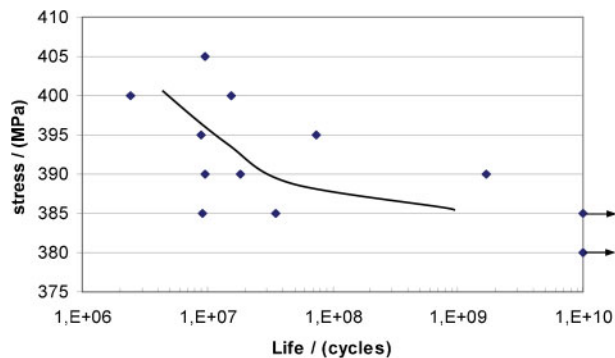
4   Gigacycle fatigue of 100C6 in torsion

increases as the shear stress amplitude decreases in the life range 10^6–10^{10} cycles, such that the life is between 380 and 390 MPa in the very high cycle regime.

Rotating bending loading

At this point, it is interesting to compare the fatigue curves in rotating bending and in tension–compression. In Japanese literature, a lot of results had been reported for JIS SUJ2 by Sakai and others.[1] It has been found by Japanese researchers that the internal failure initiation appears after a plateau more important in rotating load than in tension–compression. Although the SUJ2 is not exactly the same as NF 100C6 steel; it seems that the stepwise SN curve is common for both and therefore, more related to the rotating bending behaviour.

Whereas the SUJ2 has been tested in the authors' laboratory under tension–compression mode at 20 kHz, and no step in the SN curve could be derived. Thus, it is assumed that this step depends on the calculation of the nominal stress which is decreasing from the surface to the center to get zero for a given loading (Figs. 5 and 6).

Mechanisms of initiation

According to the technical applications, a modern approach of the fatigue of components should be divided into three domains:

  (i)   low cycle fatigue when the fatigue life is $<10^5$ cycles (bulk plasticity)
  (ii)   megacycle fatigue between 10^5 and 10^7 cycles (surface plasticity)
  (iii)   gigacycle fatigue beyond 10^7 cycles (local plasticity).

It is well known that low cycle fatigue is predicted using the Coffin–Manson law, and megacycle fatigue is related to the Wöhler curve concept. But, there is no general model for gigacycle fatigue.

Observations by SEM show that the fatigue crack initiation site for the NF 100C6 and SUJ2 bearing steels was in two typical rupture modes in surface between 10^5 and 10^6 cycles, and over 10^7 cycles inside of the specimen, principally located at non-metallic inclusions such as Al_2O_3, CaO and SiO_2, in push pull loading, and at sulphur in torsion.

For the specimens tested under the smaller cyclic stress, the internal stress concentration is due to an Al_2O_3 inclusion. In Fig. 7a, the authors find an optical dark area found by other researches. Figure 3b shows a detail of the inclusion in the centre of a fish-eye under 960 MPa cyclic stress, with some white areas; its fatigue life is up to $1·08 \times 10^8$ cycles.
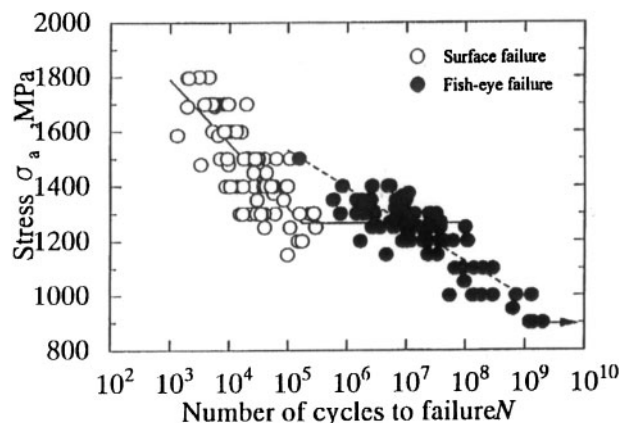

5   Gigacycle fatigue of SUJ2 in rotative bending (by Sakai et al.)[1]

Very often, some butterfly wings (Figs. 8 and 9) occur around the inclusion from which the initiation is starting in bearing steels. According some observations given in the literature,[9] it seems that the wings are the result of a transformation of the martensite in ferrite due to local shear. After polishing some scattered white areas are found beneath the fish-eye. Notice cracks along the boundary of the wing. Instability of the quenched microstructure is probably the reason of the formation of butterfly wings after a great number of cycles with a high strain rate. Comparison between damage mechanisms in rolling fatigue and in axial gigacycle fatigue is fruitful.

Thermal dissipation during fish-eye nucleation and growth

To improve quality materials, it is necessary to understand why they can fail at 10^9 cycles under small elastic loading and why the initiation may occur. The initiation phase in the gigacycle fatigue can be described in terms of a local microstructurally irreversible portion of the cumulative plastic strain. When crack initiation appears, a short crack propagates followed by a long crack. In all cases, a cyclic plastic zone around the crack occurs leading to a high thermal dissipation. So, the recording of the surface temperature of the sample during the test must allow to follow the fatigue damage and to determine the number of cycles at the crack initiation. The temperature evolution measured on the surface specimen during the tests is analysed before and during crack initiation (with a special attention to the number of cycles at initiation). At the first time, an increase in the temperature was observed just at the beginning of the test, which corresponds to the thermal dissipation in the specimen. In the same material, the temperature increases depending on the maximum stress amplitude for a given number of cycles. It should be noted that this increase in temperature at the beginning of the test is followed by a stabilisation corresponding to a balance between the mechanical energy dissipated into heat and the energy lost by convection and radiation at the specimen surface and by conduction inside the specimen. As the crack initiation occurs, it is seen that the temperature increases rapidly. From the temperature recording, the number of cycles at crack initiation can be determined. This damage phase includes crack propagation of a short crack followed by a long crack with cyclic

Courbe S-N, acier 100C6 martensitique SUJ2, 20 kHz, R =-1
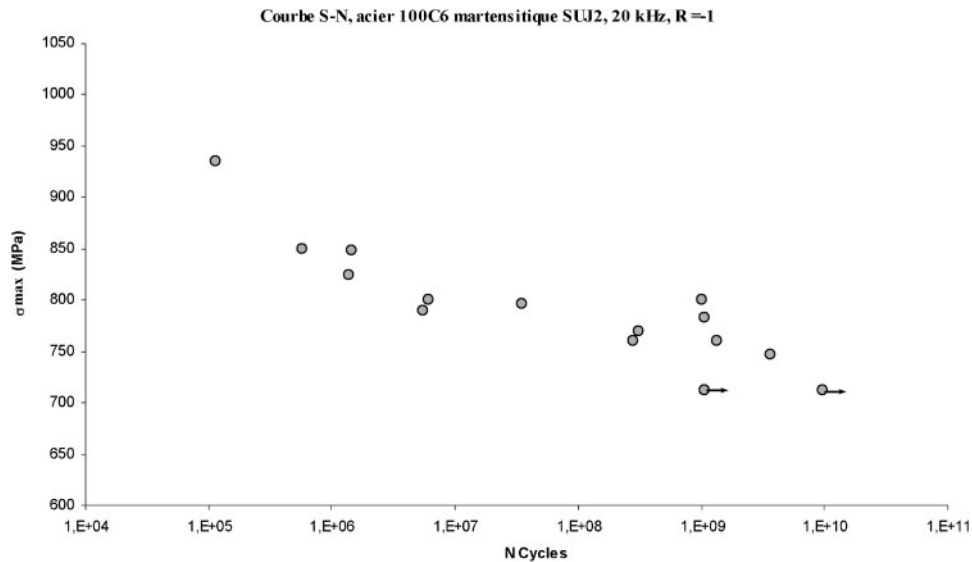
6   Gigacycle fatigue SN curve of SUJ2, tension–compression

plastic zones, ahead of the crack, which leads to high thermal dissipation. There are two difficult problems to detect experimentally the initiation in the gigacycle regime: the great number of cycles and the location beneath the surface. So, the recording of the surface temperature is a very interesting technique to determine accurately the number of cycles at initiation of the crack. In the tests performed in the present study, the number of cycles at crack initiation is >92% of the total number of cycles beyond 10^7 cycles, in agreement with the Paris–Herzberg derivative relation.

Murakami model

The Murakami model allows prediction of the material fatigue limit for materials containing three-dimensional defects, like non-metallic inclusions or porosities. The necessary imput data are: Vickers hardness of material *HV*, the defect dimension *area*$^{1/2}$ (µm) and the loading criterion *R*. Murakami based his model mainly on fatigue steel tests under rotational bending, but he affirms, it is applicable to other metals.

Murakami does not specify the number of cycles, since the model considers that the lifetime is unlimited. Previously, it has shown that the 'fatigue limit' can vary appreciably between 10^7 and 10^{10} cycles. Results from Murakami and other literature do not originate generally from high frequency fatigue tests and we can suppose that the maximum number of cycles is $<10^8$

cycles. Therefore, the necessity to predict a fatigue limit at long lifetime (gigacyclic regime) and verify the Murakami model efficiency into this regime (equation (1)), is possible using NF 100C6 bainitic data.

$$\sigma_{\mathrm{w}} = \frac{1 \cdot 56(HV + 120)}{(area^{1/2})^{1/6}} \left(\frac{1 - R}{2}\right)^{\alpha} \qquad (1)$$

where $C = 1 \cdot 56$ for the internal defects, σ_{w} is the fatigue resistance (MPa), R is the loading ratio and $\sigma = 0 \cdot 226 + HV \times 10^{-4}$

Because loading ratio is $R = -1$, equation (1) will be changed as follows

$$\sigma_{\mathrm{w}} = \frac{1 \cdot 56(HV + 120)}{(area^{1/2})^{1/6}} \qquad (2)$$

Figure 10 shows the results between the experimental results obtained by the authors and those from Murakami using NF 100C6 bainitic data representing long lifetime, where, the error percentage is between $11 \cdot 1$ and $24 \cdot 2\%$. However, by changing the internal defect constant the error can be between $0 \cdot 1$ and $5 \cdot 9\%$ using equation (3).

Figure 10 shows the modified SN curve data using NF 100C6 bainitic steel, where the difference between equations (2) and (3) can be illustrated.

$$\sigma_{\mathrm{w}} = \frac{1 \cdot 83(HV + 120)}{(area^{1/2})^{1/6}} \qquad (3)$$
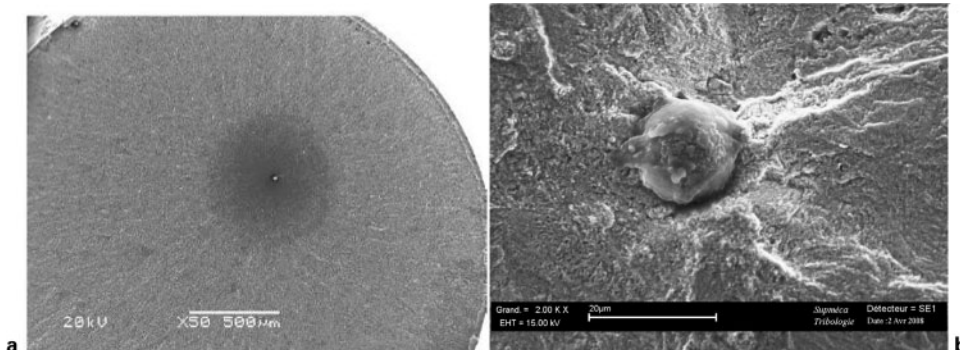
7   Fish-eye initiation in *a* bearing steel and *b* inclusion with optical dark area
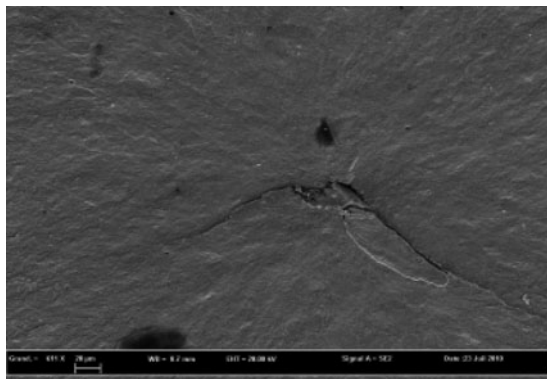
8 Center of fish-eye with butterfly wings starting from oxide
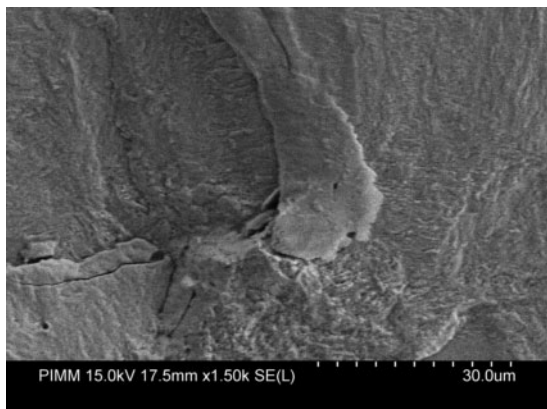

10 Murakami model apply to 100C6

It shows that the Murakami model can be useful in gigacyclic regime to predict the fatigue resistance, taking only care of inclusion size at nucleation crack.

The Murakami model is a good empirical approach to predict the fatigue strength of bearing steels depending on the defect size. However, the fatigue life that covers both crack initiation and crack growth is not evaluated. Assuming that the gigacycle fatigue is related to the fish-eye formation, it is reasonable to compute the number of cycles for propagation by the integration of the Paris–Hertzberg law applied to a circular short crack. In gigacycle fatigue regime, the geometry of the fish-eye initiation is a circle which collapses arriving at the surface of the specimen.
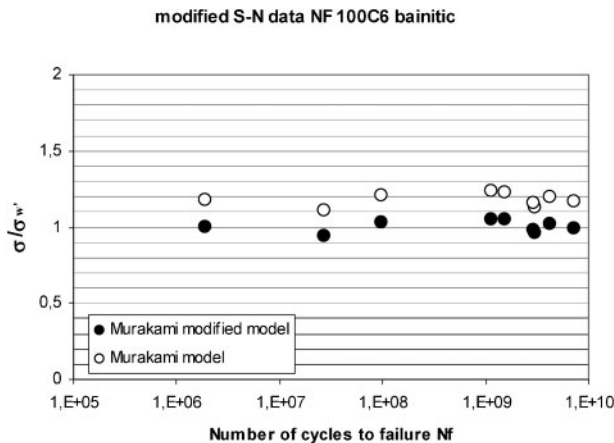
Fish-eye growth Paris–Bathias model

In order to do this, one should refer to the general behaviour pattern of the crack growth rate Paris–Hertzberg relation. It is assumed that small cracks such as those growing from small inclusions do not exhibit crack closure so these equations in terms of ΔK_{eff} apply fairly well. They form an upper limit on crack growth rates for the small cracks in the 'fish-eye' range for which crack closure is minimal.

Estimating the life for a crack of this type beginning just above threshold, it is then appropriate to consider the growth law as

9 High magnification of butterfly wings and cracks in fish-eye

$$\frac{\mathrm{d}a}{\mathrm{d}N} = b\left(\frac{\Delta K_{\text{eff}}}{Eb^{1/2}}\right)^3 \qquad (4)$$

where for the circular crack growing in a 'fish-eye', the stress intensity factor formula is

$$\Delta K = \frac{2}{\pi}\Delta\sigma(\pi a)^{1/2} \qquad (5)$$

the integration to determine the crack growth life during the fish-eye propagation is found

$$N_{\text{f}} = \frac{\pi E^2}{2(\Delta\sigma)^2} \qquad (6)$$

For the completeness of these results let us consider the number of cycles which can be considered crack growth below the threshold point. The relation becomes

$$N_{\text{f}} \cong \frac{\pi}{12}\left(\frac{E}{\Delta\sigma}\right)^2 \qquad (7)$$

Therefore, it is shown that crack growth before the threshold point is of little consequence in gigacycle fatigue.

From equation (6), it is found that the number of cycles of crack growth N_{f}, is of the order of 10^5 cycles, about three orders of magnitude smaller or much less than 1% of the total life. It means that the key problem to improve the gigacycle fatigue of bearing steels is to reduce the internal crack initiation around inclusions starting from dislocation sliding and phase transformation.

Conclusions

Experimentally it is shown that beyond 10^7 cycles, fatigue rupture can still occur in bearing steels. In some cases, the difference of fatigue resistance can decrease by 100, or even 200 MPa, between 10^6 and 10^9 cycles to failure. According to the authors' observations, the concept of an infinite fatigue life on an asymptotic SN curve is not correct. Under these conditions, a fatigue limit defined with a statistical analysis between 10^6 and 10^7 cycles cannot guarantee an infinite fatigue life. In the gigacycle fatigue range, a piezoelectric fatigue machine has been used at 20 kHz. This means that those effects of frequency and heat dissipation could be suspected. In the examples quoted, it seems that these effects are very small (the specimen temperature is $<60°C$ when the fatigue life is

$>10^7$ cycles). However, if the amount of retained austenite is $>10\%$, the heating dissipation is more important.

In bearing steels, the main factors involved in fish-eye initiation are: microstructure, residual austenite, oxide inclusion, sulphur and phase transformation.

References

1. T. Sakai: 'Review and prospects for current studies on very high cycle fatigue of metallic materials for machine structural use', Proc. 4th Int. Conf. on 'Very high cycle fatigue', Ann Arbor, MI, USA, August 2007, TMS.
2. C. Bathias and P. C. Paris: 'Gigacycle fatigue in mechanical practice'; 2004, New York, Marcel Dekker.
3. C. Bathias: 'There is no infinite fatigue life in metallic materials', *Fatigue Fract. Eng. Mater. Struct.*, 1999, **22**, 559–565.
4. C. Bathias: 'Piezo-electric fatigue testing machines and devices', Proc. 3rd Int. Conf. on 'Very high cycle fatigue', Toyko, Japan, September 2004, TMS, 472–483.
5. T. Y. Wu, J. G. Ni and C. Bathias: 'Automatic in ultrasonic fatigue machine to study low crack growth at room and high temperature', *ASTM STP*, 1993, **1231**, 598–607.
6. Q. Y. Wang, J. Y. Berard and C. Bathias: 'Gigacycle fatigue of ferrous alloys', *Fatigue Fract. Eng. Mater. Struct.*, 1999, **22**, (8), 667–672.
7. C. Bathias and J. G. Ni: 'Determination of fatigue limit between 10^5 and 10^9 cycles using an ultrasonic fatigue device', *ASTM STP*, 1993, **1211**, 151–152.
8. N. Ranc, D. Wagner and P. C. Paris: 'Study of thermal effects associated with crack propagation during very high cycle fatigue', *Acta Meter.*, 2008, **56**, 4012–4021.
9. A. Grabulov, U. Ziese and H. W. Zandergen: 'Investigation of microstructural changes within white etching area under rolling contact fatigue', Proc. 4th Int. Conf. on 'Very high cycle fatigue', Ann Arbor, MI, USA, August 2007, TMS, 219–226.